Energy, Mines and Resources Canada

Énergie, Mines et Ressources Canada

CANMET

Canada Centre for Mineral and Energy Technology

Centre canadien de la technologie des minéraux et de l'énergie

Mining Research Laboratories

Laboratoires de recherche minière

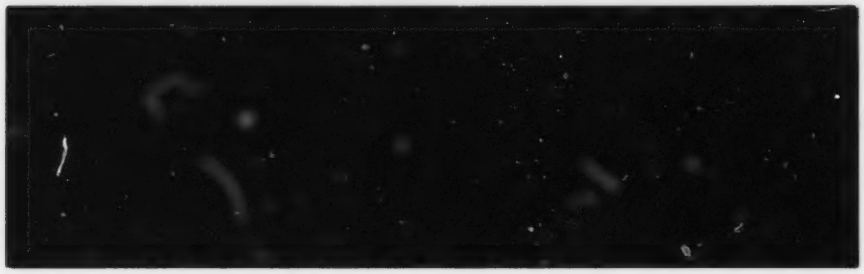

Canada

91-03595/

A LOCAL SEISMIC SURVEY AT DENISON MINE

M. PLOUFFE

ELLIOT LAKE LABORATORY

MRL 91-018 (TR) SEPTEMBER 1990

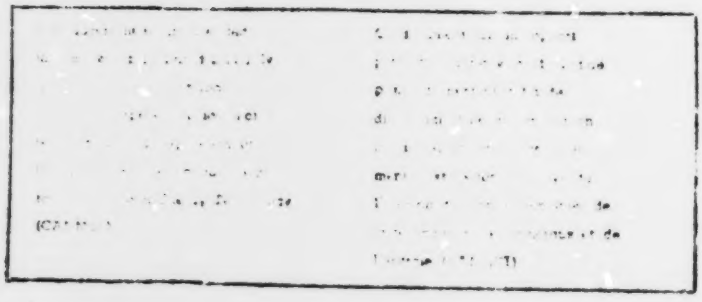

39 pp

MICROMEDIA

A LOCAL SEISMIC SURVEY AT DENISON MINE

M. Plouffe*

ABSTRACT

Denison Mine, Elliot Lake, was chosen as a site to conduct a seismic survey using a portable seismograph acquired by CANMET. During the approximate four-month period, 370 seismic events were recorded. Of that number, 342 were classified as blasts, and 28 as mining induced seismic, MIS, events, including a 1.9 m_N rockburst.

Waveform analysis was performed on these data and the results are in good agreement with those from other Northern Ontario mines.

Key words: Mining seismicity; Denison Mine; Waveform analysis.

*Seismologist, Elliot Lake Laboratory, CANMET, Energy, Mines and Resources Canada, Elliot Lake, Ontario.

UN LEVE SEISMIQUE A LA MINE DENISON

M. Plouffe*

RESUME

A la suite de l'acquisition d'un séismographe portatif par CANMET, la mine Denison fut choisie afin de conduire un levé de la séismicité locale. Trois cent soixante-dix événements furent enregistrés durant une période de quatre mois. De ce nombre, 342 résultèrent de l'enregistrement des explosions d'exploitation, et 28 furent classifiés comme événements induits liés à l'activité minière, LAM, dont un coup de toit de magnitude 1.9 m_N.

Les résultats de l'analyse conduite sur les données recueillies permettent de conclure que les événements induits liés à l'activité minière se produisant à la mine Denison se comparent bien avec d'autres enregistrés dans les mines du nord ontarien.

Mot-clés: Séismicité minière; Mine Denison; Analyse des formes d'onde.

*Séismologue, Laboratoire d'Elliot Lake, CANMET, Energie, Mines et Ressources Canada, Elliot Lake, Ontario.

CONTENTS

	Page
ABSTRACT	i
RESUME	ii
INTRODUCTION	1
SURVEY	1
INSTRUMENTATION	2
LOCATION OF THE SEISMOGRAPH	3
EVENTS RECORDED	3
LOCATION OF THE MIS EVENTS	3
MAGNITUDE OF THE MIS EVENT	4
DATA ANALYSIS	5
ATTENUATION	8
SEISMIC SOURCE PARAMETERS	9
FUTURE INVESTIGATIONS	11
ACKNOWLEDGEMENT	12
REFERENCES	12

TABLES

No.		
1.	Classification of events recorded by the PDAS-100	15
2.	List of MIS events	16
3.	List of hypocentral distances and S-P time differences	17
4.	List of seismic parameters	18
5.	Comparison between P-wave and total waveforms for some parameters	19
6.	List of seismic source parameters	20
7.	List of stress drops, source radii and slippages	21

FIGURES

1.	Map showing a general view of the Quirke II and Denison Mines with locations of the recorded MIS events and the sensor during the survey	22
2.	Distinctive signature of the blasts recorded during the survey	23
3.	The April 27, 1990 event (magnitude 1.9 m_N) as originally recorded in acceleration mode	24
4.	Relationship between S-P time difference and hypocentral distance	25
5.	Peak particle velocity as a function of magnitude from Denison Mine data compared to Spottiswoode and Hedley	26

6. Peak particle velocity as a function of scaled distance ($\frac{R}{10^{m/3}}$) 27

7. Peak particle acceleration as a function of scaled distance ($\frac{R}{10^{m/3}}$). 28

8. Relationship between seismic energy and magnitude 29

9. Ratio of the seismic energy contained in the P-wave compared to the total seismic energy 30

10. Relationship between seismic moment and magnitude 31

11. Relationship between seismic moment and corner frequency assuming a constant stress drop pattern between 0.25 and 10 MPa 32

12. Seismic moment as a function of peak acceleration parameter 33

13. Seismic moment as a function of peak velocity parameter 34

INTRODUCTION

The monitoring and subsequent analysis of the mining induced seismic (MIS) activity in Northern Ontario became a mandate of CANMET (Canada Centre of Mineral and Energy Technology) in 1984 when the Canada/Ontario/Industry Rockburst Project was inaugurated (1). In partial implementation of these objectives, CANMET supports the operation of five regional seismographic stations and five macroseismic systems in Ontario mines that are experiencing rockbursts.

In order to carry out local seismic activity surveys in the epicentral distance range not covered by these two types of networks, CANMET acquired, in 1989, a state-of-the-art portable seismograph. Associated local surveys could either contribute to aftershock surveys, coverage of activity while the micro and/or macroseismic networks are not in operation, or supplement these networks.

Denison Mine of Denison Mines Ltd. was chosen as a test site for this portable seismograph. This mine, which is located about 10 km north of the town of Elliot Lake, Ontario, has since September 1984 (2), been subjected to mining induced seismic activity.

During the survey conducted in the spring of 1990, 370 events were recorded. Of this total, 28 were classified as MIS events of which the largest was magnitude 1.9 m_N.

It was the first time that an analysis was performed by CANMET on data recorded at Denison Mine close to the seismic activity. Analysis of the data showed a close correlation with the analysis of data recorded in other Northern Ontario mines.

SURVEY

The survey was requested by both CANMET and Denison Mine to continue to test the feasibility of deploying this type of portable seismograph, and

possibly to monitor any increased seismic activity due to the presence of large quantities of water in their on-going backfill process.

The survey was conducted at Denison Mine, between February 20 and June 28, 1990. The portable seismograph recorded seismic events during this period except for a one-week interval between February 20 and 27 when due to a high threshold level no seismic activity was recorded.

INSTRUMENTATION

The seismograph used for this survey was a PDAS-100 (acronym for Portable Data Acquisition System) manufactured by Teledyne-Geotech.

During the survey, a full scale low-gain input of 2.0 V was maintained, i.e., according to calibration the maximum peak particle velocity that could be recorded was about 250 mm/s.

A trigger level was set up to have a lower threshold equivalent of 2.5% of the input (±50 mV). Therefore, all events generating a voltage higher than ±50 mV should have triggered the seismograph. However, during the first week of the survey, the trigger level was set to be equivalent to 15% of the input because of the possible high background noise generated by the nearby mining areas. As no seismic event was recorded during that period, the trigger level was lowered to 2.5% as a test level, and maintained at that level for the remainder of the survey.

The triggered events were sampled at a rate of 1000 samples per second over a maximum window length of 2 seconds.

The sensor used was a three-component surface accelerometer, model PA-20 (also manufactured by Teledyne-Geotech). This sensor houses three orthogonal Geotech Model S-110 accelerometers. The S-110 model has a full-scale output of ±2.0 times the gravitational acceleration (g). The piezoelectric devices have a frequency response ranging from 0.20 to 2000 Hz. However, for the purpose of the present analysis only frequencies ranging

between 1 and 400 Hz were utilized.

LOCATION OF THE SEISMOGRAPH

The seismograph was deployed underground within the boundary of the Denison Mine property, close to the boundary pillar between Denison Mine and Rio Algom's Quirke II Mine (Figure 1), at a depth of about 500 m.

The seismograph was located in an old lunch room in the 31st panel, 31029 stope, and the sensor was placed about 150 m from the aforementioned boundary pillar.

EVENTS RECORLED

Three hundred and seventy events were recorded by the PDAS-100 during the survey (Table 1). All of these events were also recorded by the Electro-Lab MP-250 microseismic network installed on both sides of the boundary pillar, as later verified by the mine operator.

The majority of recorded events were due to blasting (Table 1). The percentage of blasts over the total number of recorded events (92%) was relatively high. This could be explained by the fact that, during the period of recording, mining of the 'Upper Reef' of Denison Mine was being undertaken approximately 200 m from the sensor.

Figure 2 shows the usual signatures of blasts as recorded by the PDAS-100 during the survey. These distinctive signatures are introduced by the shooting pattern and delay parameters (3).

LOCATION OF THE MIS EVENTS

A total of 28 events recorded by the PDAS-100 were classified as mining-induced seismic events (Table 1). Of this total, accurate locations could not be determined for three events (Table 2) - locations are usually determined using the MP-250 network data. The main reason for the uncertain

epicentres is that they occurred outside the array. As the microseismic network is almost planar, the location of MIS occurring in the hanging wall or footwall is only approximate.

Using the arrival times as recorded by the MP-250 network, the locations were calculated using a BLOCK source-location technique (4). The BLOCK method calculates the source location using the smallest value of an objective function as follows:

$$F(X,Y,Z) = [t_i - t_1) - (t_i^c - t_1^c)]^2 \qquad \text{Eq 1a}$$

where,

$$t_i^c = [(X-a_i)^2 + (Y-b_i)^2 + (Z-c_i)^2]^{1/2}/V_i \qquad \text{Eq 1b}$$

t_i = arrival time for the ith geophone

a_i, b_i & c_i = ith geophone coordinates

X, Y & Z = coordinates of the trial point

V_i = average velocity from the source to the ith geophone.

Locations found by using the BLOCK method are marked on Figure 1 according to the numerical order of the MIS events as listed on Table 2. The location of two events was not determined due to the poor data recorded by the MP-250.

MAGNITUDE OF THE MIS EVENTS

Magnitudes for seismic events are calculated through S-wave amplitude measurements recorded by the National Seismograph Network. The network stations closest to Elliot Lake are three seismograph stations of the Sudbury Local Telemetered Network (SLTN) which are located at a distance of about 100 km. Only the largest events originating from the Elliot Lake mines could be recorded by SLTN, the lower magnitude threshold being around 1.7 m_N.

For lower magnitude events, a seismograph station installed at Elliot Lake to record the local seismic activity is used. This seismograph is located about 10 km from the local mines. This station was calibrated against the national network in 1987 (5). An empirical scale based on the time

duration of the seismic signal was then developed and an equivalent magnitude down to 0.8 m_N could be determined.

In the present survey of the 28 MIS events, 16 were not recorded by the Elliot Lake seismograph or the Sudbury Local Telemetered Network. Hence, the magnitude of these events could not be determined, however, a magnitude lower than 0.8 could be attributed to them (Table 2).

Of the remaining 12 MIS events, only 2 were also recorded by the Sudbury Local Telemetered Network (SLTN). The magnitude range of these 12 events was between 0.8 and 1.9 m_N (Table 2). The magnitude values are based on the empirical magnitude scale defined by Rochon (5), except for the two recorded by SLTN. The 1.9 m_N (Figure 3) event was the second largest recorded at Denison Mine since the beginning of 1990; the largest being a 2.1 m_N on February 13, 1990.

DATA ANALYSIS

The digitized signals of the selected events were analyzed first to determine travel path parameters such as peak particle acceleration and velocity, seismic energy, and P- and S-wave arrivals. An analysis of the seismic source parameters using Brune's model (6,7) was carried out in the frequency domain.

No analysis was carried out on the unlocated March 14, 1990 event as it occurred during a blasting time, causing the signature of this MIS event to be hidden by the background noise from the blasts.

For the other unlocated events, the time difference between S- and P-wave arrivals was compared with one of the located events to increase the number of events studied. Table 3 lists the hypocentral distances of the events against their S- and P-wave time differences, and Figure 4 shows this relationship assumed as a uniform velocity:

$$\text{Distance (m)} = 9 \times \text{time difference (msec)} + 40 \qquad \text{Eq 2}$$

Hypocentral distances ranged from 180 to 1110 m approximately.

The parametric values of the unlocated events were not used to determine any empirical relationship.

A. PEAK PARTICLE VELOCITY

The vector sum peak particle velocities (PPV) measured range between 0.10 and 3.50 mm/s (Table 4). These values are consistent with the trend given by Hedley (8) for Ontario mines:

$$\log(R\underline{v}) = 0.63\ M - 1.33 \qquad \text{Eq 3}$$

where, M = earthquake magnitude

R = hypocentral distance in m,

$\underline{v}$ = peak particle velocity in m/s,

This relationship uses the same empirical format as Spottiswoode (9) and Gibbon (10), who derived this relationship for the South African gold mines. Figure 5 shows that data from Denison Mine follow the same trend, albeit much below the trend defined by Spottiswoode (9).

Hedley (8) also defined this relationship in an equivalent format used for blasting:

$$\underline{v} = 4000\ \left(\frac{R}{10^{M/3}}\right)^{-1.6} \qquad \text{Eq 4}$$

where, the attenuation factor of -1.6 is calculated using data recorded on ground surface from Rio Algom's Quirke II mine at Elliot Lake, and underground data from Inco's Creighton Mine, Sudbury.

Using the data from Denison Mine in the above relationship, an attenuation coefficient of -3.0 is deduced. This lower value could be attributed to either shorted hypocentral distances, higher frequencies, a combination of both, or scattering, suggesting that the attenuating effects of the fractured zones and the surrounding mining zones could be more important under these circumstances.

However, Hedley's relationship could be used as a first approximation

depicted in Figures 6 and 7 where the ratio of R, the distance, over $10^{M/3}$ is plotted against the velocity or the acceleration.

B. PEAK PARTICLE ACCELERATION

The vector sum peak particle accelerations (PPA) measured during the survey range from about 100 mm/s^2 (about 1% of the gravitational acceleration, g) to 1330 mm/s^2 (14% of g) for the 1.9 m_N event (Table 4).

Hedley (11) defined a relationship between peak particle acceleration (a), magnitude, and distance in a format equivalent to that used for blasting:

$$a = 30 \left(\frac{R}{10^{M/3}}\right)^{-1.33} \qquad \text{Eq 5}$$

The attenuation factor of -1.33 is calculated using data recorded at Creighton and Falconbridge's Strathcona mines, Sudbury. An attenuation coefficient of -2.6 (Figure 7) can be found using only the data from Denison Mine. The same argument as used for the attenuation factor for peak particle velocities could be used for peak particle accelerations, i.e., the attenuating effects of the nearby fractured zones and the surrounding mining zones could be more important than previously determined.

For all events the maximum peak particle acceleration is found in the S-wave (Table 5). This result apparently confirms conventional earthquake seismicity theory in that the peak particle acceleration in the P-wave could be about three-fifths that of the acceleration recorded in the S-wave. The averaged PPA found for the P-wave is about half that of the PPA recorded in the S-wave.

C. SEISMIC ENERGY

Cook (12) defined the energy radiated from a seismic source, Es, in an elastic medium as:

$$Es = 4 \pi R^2 \rho \left(\alpha \int^{Tp} Vp^2 \, dt + \beta \int^{Ts} Vs^2 \, dt\right) \qquad \text{Eq 6}$$

where, ρ = density

α or β = the compressional or shear wave velocity

R = hypocentral distance

Vp or Vs = ground velocity of P- or S-wave

Tp or Ts = duration of the seismic waves in P or S phases.

The total seismic energies listed in Table 4 are the sum of each axis as these axes were orthogonally deployed.

These seismic energy values have the same trend as that defined by Hedley (13) (Figure 8). This could confirm a similar deviation from a linearly elastic behaviour to the one observed by Hedley at Quirke II Mine.

Figure 9 shows seismic energy of the P-wave, E_p, which varies between 2% and 6% of the total seismic energy, E_T, contour lines, with an average value for all MIS events of about 4%. This deduction contradicts the observations made by Hedley (13). However, the energy found in the P-wave cannot be ignored. These results may be compatible with the results by both Cook (12), and Spottiswoode and McGarr (14), who observed in mine tremors in South Africa that about 10% of the seismic energy can be found in the P-wave.

The small ratio of E_p/E_T could be explained by the kind of focal mechanisms, non-double couple, found from Quirke and Denison Mines data by Chen (15).

ATTENUATION

Seismic source parameters are usually determined through spectral analysis, but these spectra should be properly corrected for the attenuation caused by the heterogeneities of the rock causing the attenuation of the waveforms while propagating through the ground. The attenuation rate is conventionally expressed by an average quality factor, Q.

The quality factor, Q, was determined using the technique of Tsujiura (16) whose straightforward method consists of taking the natural logarithm of the ratio of two spectral amplitudes (Ω) at frequencies greater than the corner frequency thus:

$$\ln [\Omega(f_2)/(\Omega(f_1)] = \pi (f_2-f_1) \tau^* \quad \text{Eq 7}$$

is used to compute τ^* which is the attenuation operator. This attentuation operator is equal to the total travel time of the wave divided by a mean Q (17,18). The spectral amplitudes are thus corrected by multiplying each value by the exponential term $\exp(\pi f \tau^*)$ at each frequency f.

The average factor, Q, found for the shear wave for Denison Mine is 10. This may reflect the high attenuation that could be found in a highly fractured and mined region surrounding the sensor.

SEISMIC SOURCE PARAMETERS

Seismic source parameters are based on the shear waves only. A variable window was used to bind the shear waves and minimize contribution from crustal reverberations. The length varies according to the hypocentral distances and the coda of the signal, and ranged between 100 and 1000 msec.

A correction was tried on the shear wave spectra using a τ^* of about 0.007. But as the correction factor was flattening the spectral density curve, and even increasing the spectra values for high frequencies, it became very difficult to peg the corner frequencies so no attentuation correction was applied in the present study for corner frequency calculations. This tendency could be explained by the fact that a Q value of 10 represents an average value and a much lower value should have been applied.

To obtain a final result for each event, plateau values for each axis were combined as vector sums (19), and corner frequencies were averaged (20). On the basis of these plateau and corner frequency values, seismic moment, source radius, stress drop, and average slippage are calculated.

The following equations are derived from Brune's model (6,7), and are a convenient formulation for estimating mining-induced seismic source parameters. The equations to calculate the seismic moment (Mo), the source radius (Ro), the stress drop ($\Delta\sigma$), and the average slippage (ψa) are:

$$Mo = \frac{4 \pi c^3 \rho R \Omega o}{F\infty} \qquad \text{Eq 8}$$

$$Ro = \frac{K_B \beta}{2 \pi fo} \qquad \text{Eq 9}$$

$$\Delta\sigma = \frac{7 Mo}{16 Ro^3} \qquad \text{Eq 10}$$

$$\psi a = \frac{16 \Delta\sigma Ro}{7 \pi G} \qquad \text{Eq 11}$$

where, c = α or β the compressional, or shear wave velocity, respectively

ρ = density (2700 kg/m^3)

G = shear modulus = $\rho \beta^2$

K_B = source model constant (2.34)

R = hypocentral distance

Ωo = low frequency spectral density level

$F\infty$ = average radiation pattern factor (0.57)

fo = corner frequency.

Equations 9, 10 and 11 show that seismic source parameters are related to corner frequency and seismic moment (6,7); these equations apply to a circular fault model. These relationships associated with seismic moment are important when comparing small events with larger ones when no magnitude can be attributed to some events.

Tables 6 and 7 list the seismic source parameters found in this analysis.

A. SEISMIC MOMENT

The seismic moment is a convenient measure of the size of any seismic event. It is related to fault dimensions and slippage along that fault. The concept of seismic moment is restricted to fault-slip events.

Seismic moment is usually compared to magnitude. Hasegawa (21) determined an empirical relationship between seismic moment and magnitude for earthquakes in the Canadian Shield:

$$\log Mo = 0.94 Mn + 1.32 \text{ (GN-m)} \qquad \text{Eq 12}$$

Semadeni (20) and Hedley (13) present evidence to show that this relationship is also valid for mining-induced fault-slip like seismic events in Northern Ontario. However, Figure 10 shows that the 1990 Denison events follow a similar trend to Hasegawa's but lower. This could be explained by the pillar-burst type of mechanisms suggested by MIS events in the Quirke II and Denison mines, as non-double couple events are measured by dipole strength instead of seismic moment (22).

B. SCALING RELATIONSHIPS

A constant stress drop pattern has been found for some earthquakes and mine tremors, although several recent studies are finding variable stress drops (17). This implies that corner frequency decreases as seismic moment increases, as shown by Figure 11. Straight lines are contours of constant stress drop. The majority of data falls within a constant stress drop interval of 0.25 to 10 MPa.

The other source parameters vary noticeably. The source radii vary between 10 and 35 m, while the average slippages range from 0.05 to 3 mm (Table 7).

Regardless of whether this stress drop is constant or not, other empirical moment-related relationships can be found. The peak velocity parameter ($R_{\underline{v}}$) should scale according to $Mo^{1/3}$ (23), and the peak acceleration parameter ($\rho R\underline{a}$) should be independent of seismic moment.

Figures 12 and 13 show that these two relationships contradict the Denison 1990 data. The peak acceleration parameters (Figure 12), despite scatter, appear dependent on seismic moment ($Mo^{2/3}$), and the peak velocity parameters (Figure 13) seem to fit well with the seismic moment to the four-fifth power. Each relationship is indicated by the straight line on both graphs.

FUTURE INVESTIGATIONS

These preliminary results introduced some interesting features of mining-induced tremors that should be addressed in subsequent studies.

Studies on the incident waves very near the source before the scattering effects become significant should provide more information on the source itself. The low percentage of seismic energy found in the P-wave compared to results from other Northern Ontario mines, and the comparison between dipole strength and seismic moment should also be investigated. The near-field hypocentral distances, the pillar-burst type of focal mechanisms, and the highly fractured and mined zones surrounding the sensor could explain the differences between the results from this survey and surveys from other Northern Ontario mines. More comparative studies should be conducted.

However, a broadening range of data is required to shed more light on subtle differences between mining-induced tremors themselves and natural earthquakes.

ACKNOWLEDGEMENT

The author would like to thank the Denison Mine's management and mining operators, especially Mr. Chris Pritchard who gave him all the information needed.

The author wishes to thank Dr. Henry Hasegawa, Geophysics Division, Geological Survey of Canada, and Dr. Parviz Mottahed, Section Head of the Mining Technology Group, Elliot Lake Laboratory, for their critical reading of this manuscript.

REFERENCES

1. Brehaut, C.H. and Hedley, D.G.F., "1986-1987 annual report of the Canada/Ontario/Industry rockburst project"; Special Report SP87-7E, CANMET, Energy, Mines and Resources Canada, 1987.

2. Hedley, D.G.F. and Wetmiller, R.J., "Rockbursts in Ontario mines during 1984"; Special Report SP85-5, CANMET, Energy, Mines and Resources Canada 1985.

3. Smith, A.T., "High-frequency seismic observations and models of chemical explosions: implications for the discrimination of ripple-fired mining blasts"; Bull Seismol Soc Am, vol. 79, No. 4, pp. 1089-1110, August 1989.

4. Niewiadomski, J., "Source-location techniques using P-wave arrivals"; Special Report SP86-15E, CANMET, Energy, Mines and Resources Canada, 1986.

5. Rochon, P. and Hedley, D.G.F., "Magnitude scaling of rockbursts at Elliot Lake"; Division Report MRL 87-156(TR), CANMET, Energy, Mines and Resources Canada, 1987.

6. Brune, J.N., "Tectonic stress and spectra of seismic shear waves from earthquakes"; J Geophys Res, vol. 75, No. 26, pp. 4997-5009, Sept. 1989.

7. Brune, J.N., "Correction", J Geophys Res, vol. 76, p. 5002, 1971.

8. Hedley, D.G.F., "Peak particle velocity for rockbursts in some Ontario mines"; Proc 2nd Int Symp on Rockbursts and Seismicity in Mines, pp. 503-512, Minneapolis, June 1988.

9. Spottiswoode, S.M., "Underground seismic networks and safety"; Monitoring for Safety in Geotechnical Engineering, SANGORM, 1984.

10. Gibbon, G.J., De Kock, A., and Mokebe, J., "Monitoring of peak particle velocity during rockbursts"; Proc 8th West Virginia University Int. Mining Electrotechnology Conf, Morgantown, WV, 1986.

11. Hedley, D.G.F., "A five year review of the Canada/Ontario/Industry rockburst project"; Special Report SP90- (in preparation), CANMET, Energy, Mines and Resources Canada, 1990.

12. Cook, N.G.W., "Application of seismic techniques to problems in rock mechanics"; Int J Rock Mech & Min Sci, vol. 1, pp. 169-179, 1964.

13. Hedley, D.G.F., "Rockburst handbook"; Special Report SP89-004 (in

preparation), CANMET, Energy, Mines and Resources Canada, 1991.

14. Spottiswoode, S.M. and McGarr, A., "Source parameters of tremors in a deep level gold mine"; Bull Seismol Am, vol. 65, pp. 93-112, February 1975.

15. Chen, S., "Further study on source parameters at Quirke Mine, Elliot Lake, Ontario"; Division Report 91- (in preparation), CANMET, Energy, Mines and Resources Canada, 1991.

16. Tsujiura, M., "Frequency analysis of seismic waves, 1"; Bull Earthquake Res Instit, Tokyo University, vol. 44, pp. 873-891, 1966.

17. Gibowicz, S.J., "The mechanism of seismic events induced by mining: a review"; Proc 2nd Int Symp on Rockbursts and Seismicity in Mines, Minneapolis, June 1988.

18. Frankel, A., "The effects of attenuation and site response on the spectra of microearthquakes in the northeastern Caribbean"; Bull Seismol Soc Am, vol. 72, pp. 1379-1402, 1982.

19. McGarr, A., Bicknell, J., Sembera, E. and Green R.W.E., "Analysis of exceptionally large tremors in two gold mining districts of South Africa"; Fred Leighton Memorial Workshop on Mining Induced Seismicity, Montreal, 1987.

20. Semadeni, T.J., Rochon, P. and Niewiadomski, J., "Waveform analysis of mine-induced seismic events recorded at Rio Algom's Quirke Mine"; Proc 2nd Int Symp on Rockbursts and Seismicity in Mines, pp. 267-279, Minneapolis, June 1988.

21. Hasegawa, H.S., "Lg spectra of local earthquakes recorded by the Eastern Canada Telemetered Network and spectral scaling"; Bull Seismol Soc Am, vol. 73, pp. 1041-1061, 1983.

22. Hasegawa, H.S., "Surface and body-wave spectra of CANNIKIN and shallow Aleutian earthquakes"; Bull Seismol Soc Am, vol. 63, pp. 1202-1225, 1973.

23. McGarr, A., "Scaling of ground motion parameters, state of stress, and focal depth"; J Geophys Res, vol. 89, pp. 6969-6979, 1984.

Table 1 - Classification of events recorded by the PDAS-100

Month	Total	Blasts	MIS
February	9	9	
March	107	104	3
April	178	158	20
May	34	33	1
June	42	38	4
Total:	370	342	28

Table 2 - List of MIS events

No.	Date 1990	Julian Date	Local Time	Location	Magnitude m_N
1	March 13	072	04:54	Location calculated	
2	" 14	073	04:18	No location	1.1
3	" 26	085	20:59	Location calculated	1.2
4	April 03	093	17:12	Location calculated	
5	" 16	106	10:16	" "	
6	" 19	109	07:43	" "	
7	" 19	109	15:04	" "	
8	" 21	111	16:17	" "	1.1
9	" 21	111	16:22	" "	0.8
10	" 22	112	22:08	" "	
11	" 23	113	23:51	No location	0.9
12	" 23	113	23:52	Location calculated	1.8**
13	" 23	113	23:52	No location	
14	" 24	114	00:45	Location calculated	0.8
15	" 24	114	01:36	" "	
16	" 24	114	08:22	" "	
17	" 25	115	12:21	" "	
18	" 26	116	19:30	" "	
19	" 27	117	00:04	" "	
20	" 27	117	02:24	" "	1.9**
21	" 27	117	05:03	" "	0.8
22	" 27	117	15:23	" "	0.8
23	" 29	119	12:17	" "	
24	May 19	139	08:02	Location calculated	1.5
25	June 01	152	15:54	Location calculated	
26	" 13	164	16:15	" "	
27	" 24	175	05:01	" "	0.8
28	" 28	179	07:28	" "	

**Magnitudes calculated with SLTN data.

Table 3 - List of hypocentral distances and S- P-time differences

Date 1990	Local Time	Distance (m)	Time Diff. (m/sec)
March 13	04:54	246	28
" 26	20:59	1116	120
April 03	17:12	198	23
" 16	10:16	189	20
" 19	07:43	263	36
" 19	15:04	267	40
" 21	16:17	250	32
" 21	16:22	256	27
" 22	22:08	247	33
" 23*	23:51	323	41
" 23	23:52	263	42
" 23*	23:52	314	40
" 24	00:45	243	33
" 24	01:36	286	30
" 24	08:22	237	40
" 25	12:21	279	33
" 26	19:30	246	30
" 27	00:04	302	37
" 27	02:24	433	60
" 27	05:03	883	111
" 27	15:23	388	55
" 29	12:17	230	28
May 19	08:02	531	67
June 01	15:54	180	39
" 13	16:15	653	61
" 24	05:01	389	56
" 28	07:28	265	32

* Unlocated events.

Table 4 - List of seismic parameters

Date 1990	Local Time	Seismic Energy (kJ)	PPA (mm/s^2)	PPV (mm/s)
March 13	04:54	11	235	0.25
" 26	20:59	554	108	0.19
April 03	17:12	8	227	0.31
" 16	10:16	11	367	0.22
" 19	07:43	34	312	0.35
" 19	15:04	55	450	0.48
" 21	16:17	522	806	1.54
" 21	16:22	128	480	0.73
" 22	22:08	9	258	0.22
" 23*	23:51	178	520	0.64
" 23	23:52	6731	1153	3.27
" 23*	23:52	1223	136	0.61
" 24	00:45	761	626	1.30
" 24	01:36	87	892	0.71
" 24	08:22	56	226	0.37
" 25	12:21	21	302	0.20
" 26	19:30	5	214	0.16
" 27	00:04	15	104	0.14
" 27	02:24	8771	1332	3.51
" 27	05:03	281	121	0.20
" 27	15:23	76	206	0.30
" 29	12:17	13	219	0.24
May 19	08:02	975	272	0.76
June 01	15:54	12	243	0.36
" 13	16:15	148	212	0.20
" 24	05:01	36	269	0.29
" 28	07:28	2	131	0.11

* Unlocated events.

Table 5 - Comparison between P-wave and total waveforms for some parameters

Date 1990	Local Time	Seismic Energy (%)	PPA (%)	PPV (%)
March 13	04:54	4	52	42
" 26	20:59	5	37	45
April 03	17:12	4	54	40
" 16	10:16	2	50	46
" 19	07:43	4	40	38
" 19	15:04	6	48	46
" 21	16:17	5	58	54
" 21	16:22	4	40	41
" 22	22:08	5	41	47
" 23*	23:51	9	62	61
" 23	23:52	2	50	38
" 23*	23:52	4	34	62
" 24	00:45	2	54	52
" 24	01:36	2	23	21
" 24	08:22	2	62	43
" 25	12:21	2	45	51
" 26	19:30	7	40	59
" 27	00:04	1	77	36
" 27	02:24	3	37	20
" 27	05:03	1	38	30
" 27	15:23	4	76	47
" 29	12:17	2	30	36
May 19	08:02	3	43	28
June 01	15:54	9	92	79
" 13	16:15	3	40	47
" 24	05:01	5	28	32
" 28	07:28	5	19	24

* Unlocated events.

Table 6 - List of seismic source parameters

Date 1990	Local Time	Corner Frequency (Hz)	Moment (GN-m)
March 13	04:54	101	2
" 26	20:59	48	55
April 03	17:12	72	6
" 16	10:16	108	1
" 19	07:43	60	8
" 19	15:04	72	14
" 21	16:17	61	25
" 21	16:22	87	17
" 22	22:08	108	7
" 23*	23:51	78	21
" 23	23:52	70	110
" 23*	23:52	89	4
" 24	00:45	74	46
" 24	01:36	99	12
" 24	08:22	81	4
" 25	12:21	119	3
" 26	19:30	140	1
" 27	00:04	89	2
" 27	02:24	42	139
" 27	05:03	51	27
" 27	15:23	113	7
" 29	12:17	110	3
May 19	08:02	66	60
June 01	15:54	95	5
" 13	16:15	117	18
" 24	05:01	64	13
" 28	07:28	122	1

* Unlocated events.

Table 7 - List of stress drops, source radii and slippages

Date 1990	Local Time	Stress Drop (kPa)	Source Radius (m)	Slippage (mm)
March 13	04:54	350	13	0.10
" 26	20:59	1077	28	0.60
April 03	17:12	358	19	0.10
" 16	10:16	195	13	0.05
" 19	07:43	302	23	0.10
" 19	15:04	939	19	0.40
" 21	16:17	972	22	0.40
" 21	16:22	1950	16	0.60
" 22	22:08	1448	13	0.40
" 23*	23:51	1728	17	0.60
" 23	23:52	6456	20	3.00
" 23*	23:52	487	15	0.10
" 24	00:45	3234	18	1.00
" 24	01:36	2038	14	0.60
" 24	08:22	368	17	0.10
" 25	12:21	751	11	0.20
" 26	19:30	513	10	0.10
" 27	00:04	300	15	0.09
" 27	02:24	1747	33	1.00
" 27	05:03	642	26	0.30
" 27	15:23	1628	12	0.40
" 29	12:17	617	12	0.20
May 19	08:02	2982	21	1.00
June 01	15:54	813	14	0.20
" 13	16:15	4950	12	1.00
" 24	05:01	585	21	0.30
" 28	07:28	421	11	0.09

* Unlocated events.

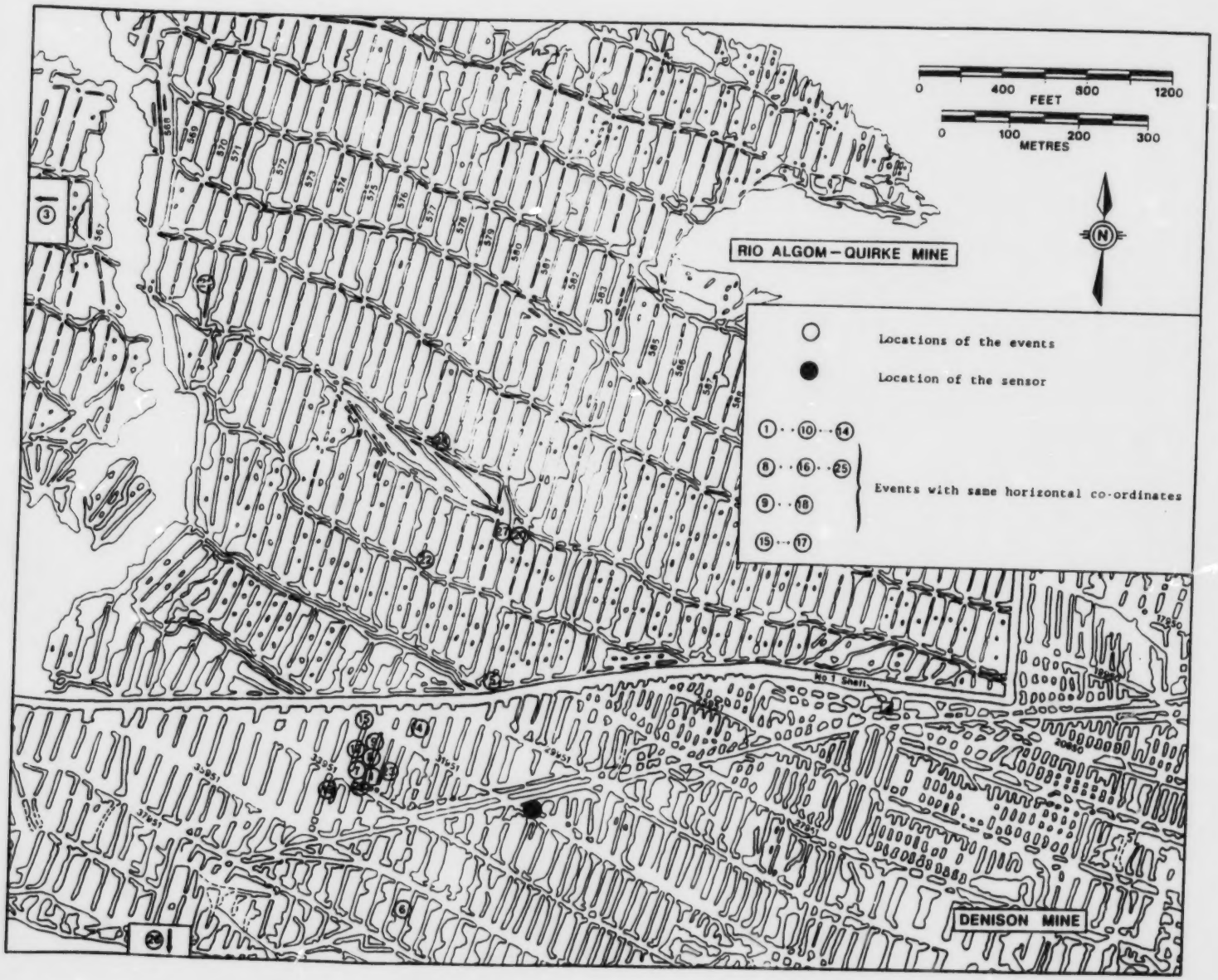

Fig. 1 - Map showing a general view of the Quirke II and Denison Mines with locations of the recorded MIS events and the sensor during the survey.

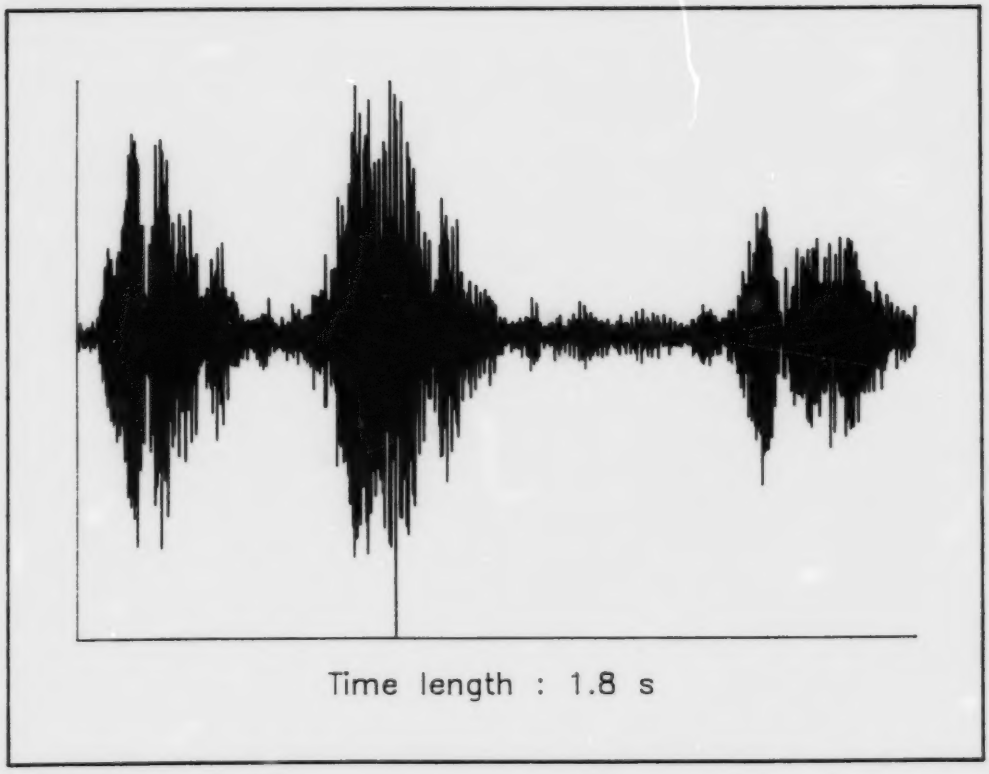

Fig. 2 - Distinctive signature of the blasts recorded during the survey.

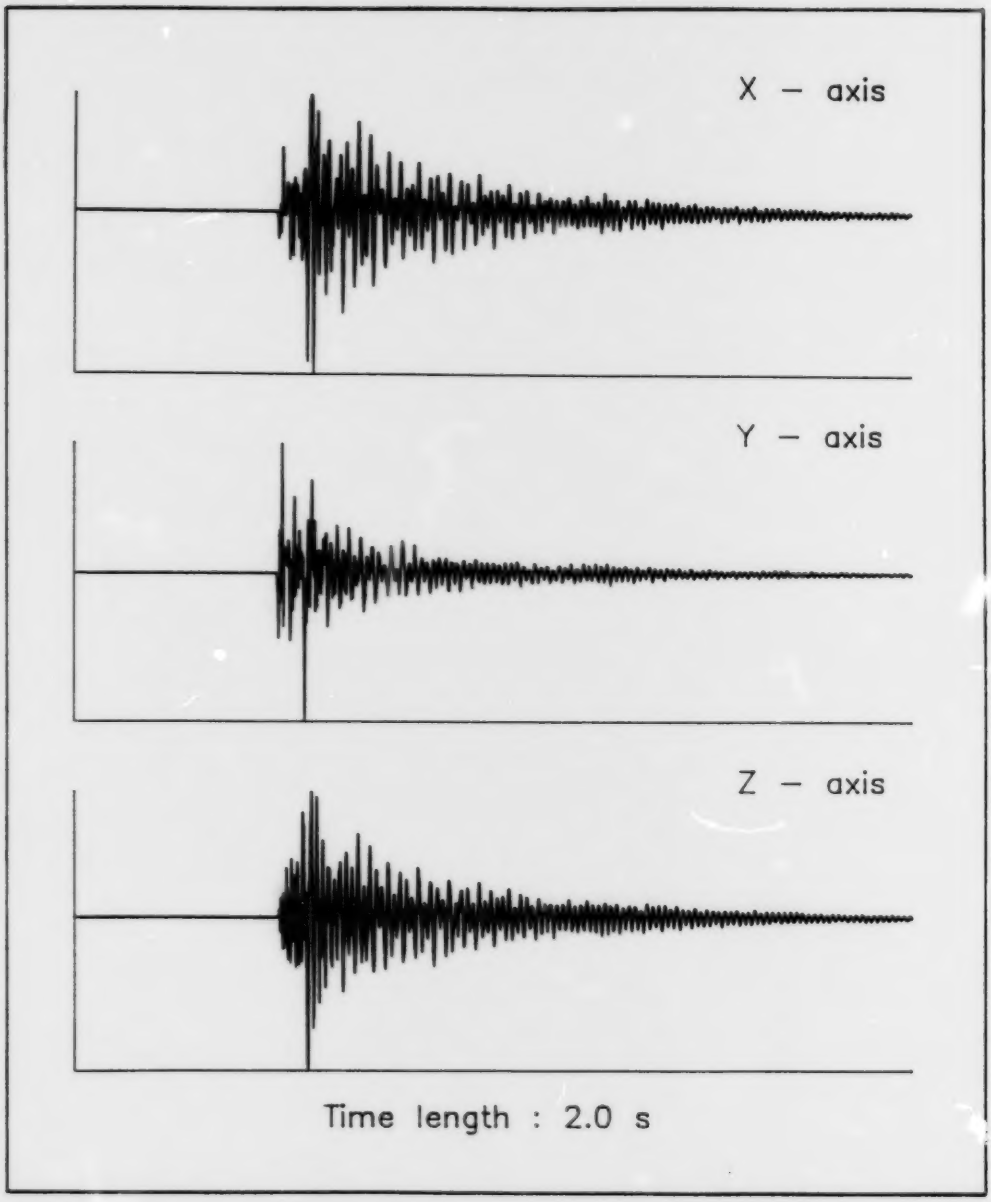

Fig. 3 - The April 27, 1990 event (magnitude 1.9 m_N) as originally recorded in acceleration mode.

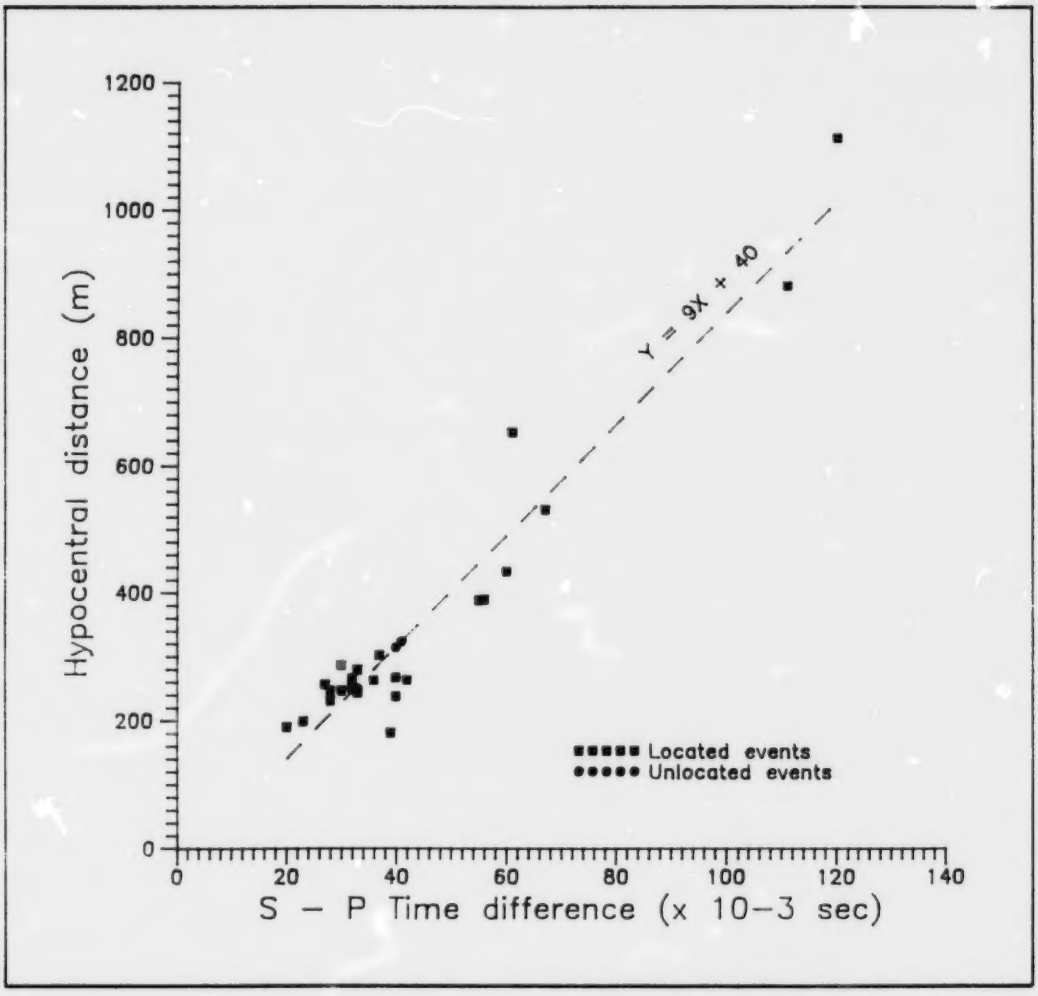

Fig. 4 - Relationship between S- P-time difference and hypocentral distance.

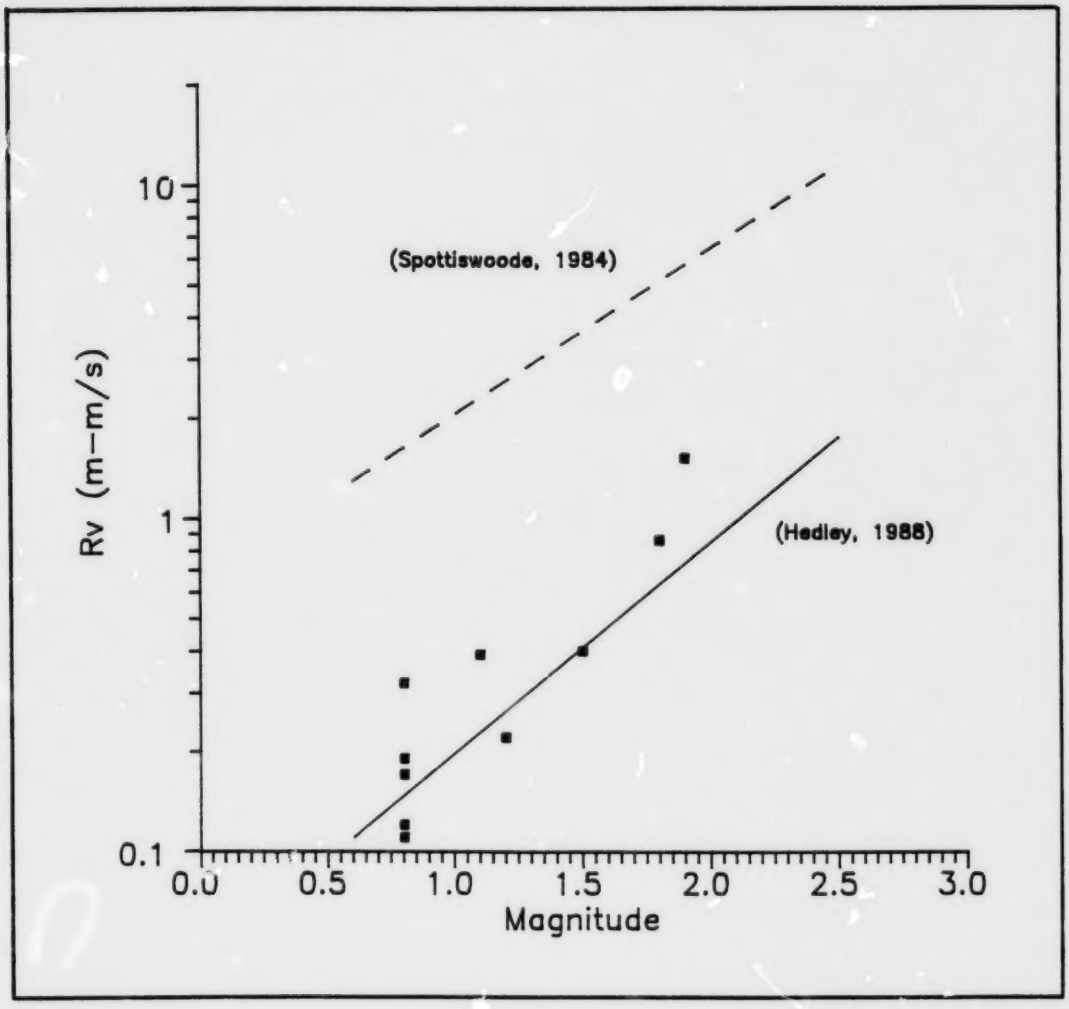

Fig. 5 - Peak particle velocity as a function of magnitude from Denison Mine data compared to Spottiswoode and Hedley.

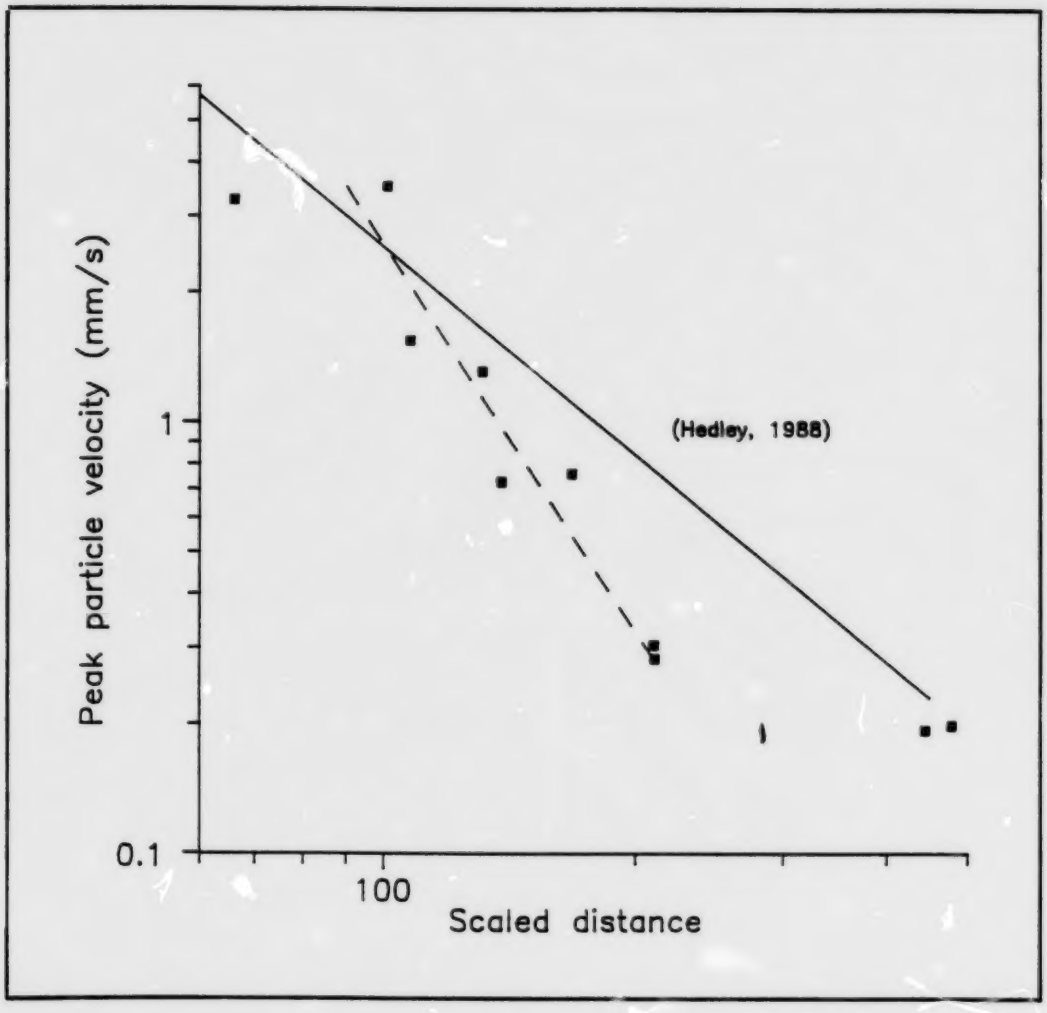

Fig. 6 - Peak particle velocity as a function of scaled distance $(\frac{R}{10^{m/3}})$.

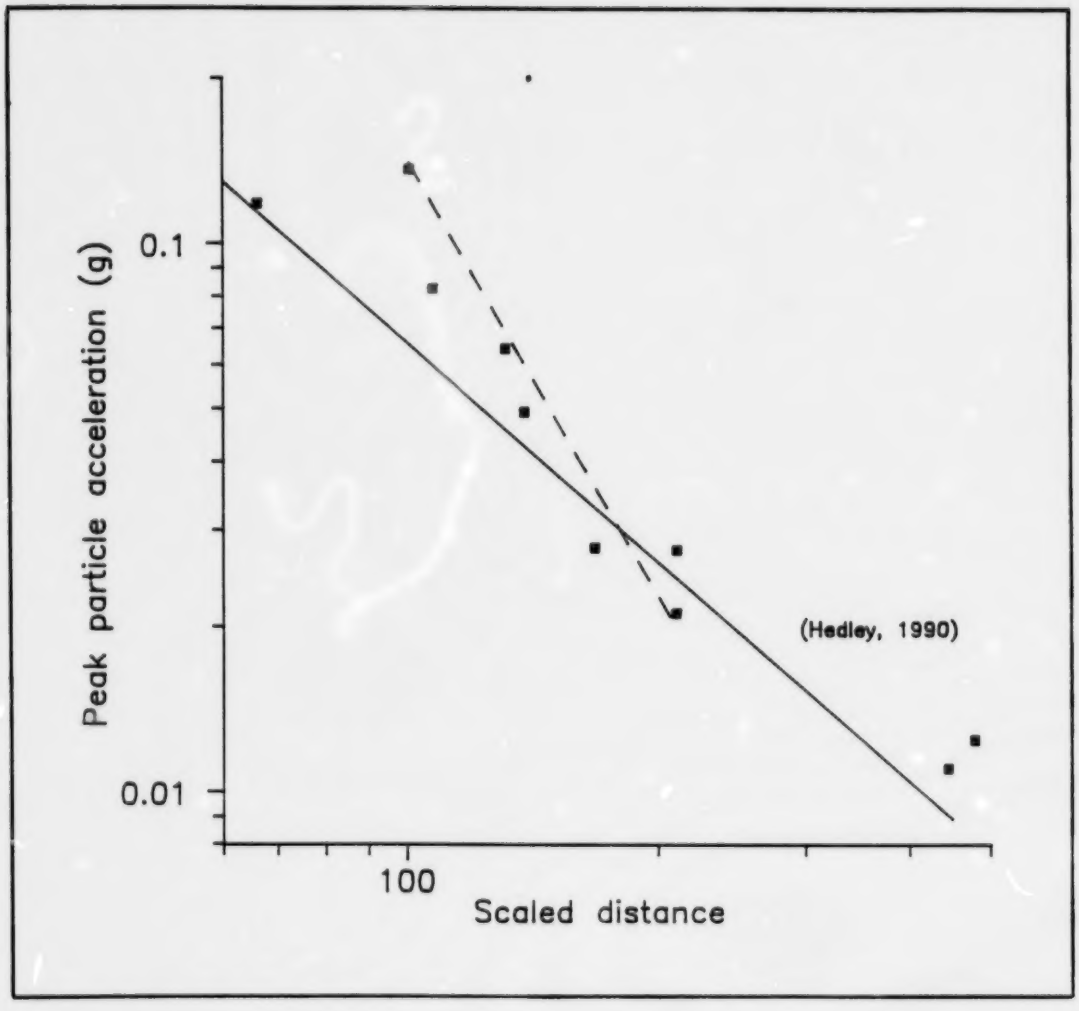

Fig. 7 - Peak particle acceleration as a function of scaled distance ($\frac{R}{10^{m/3}}$).

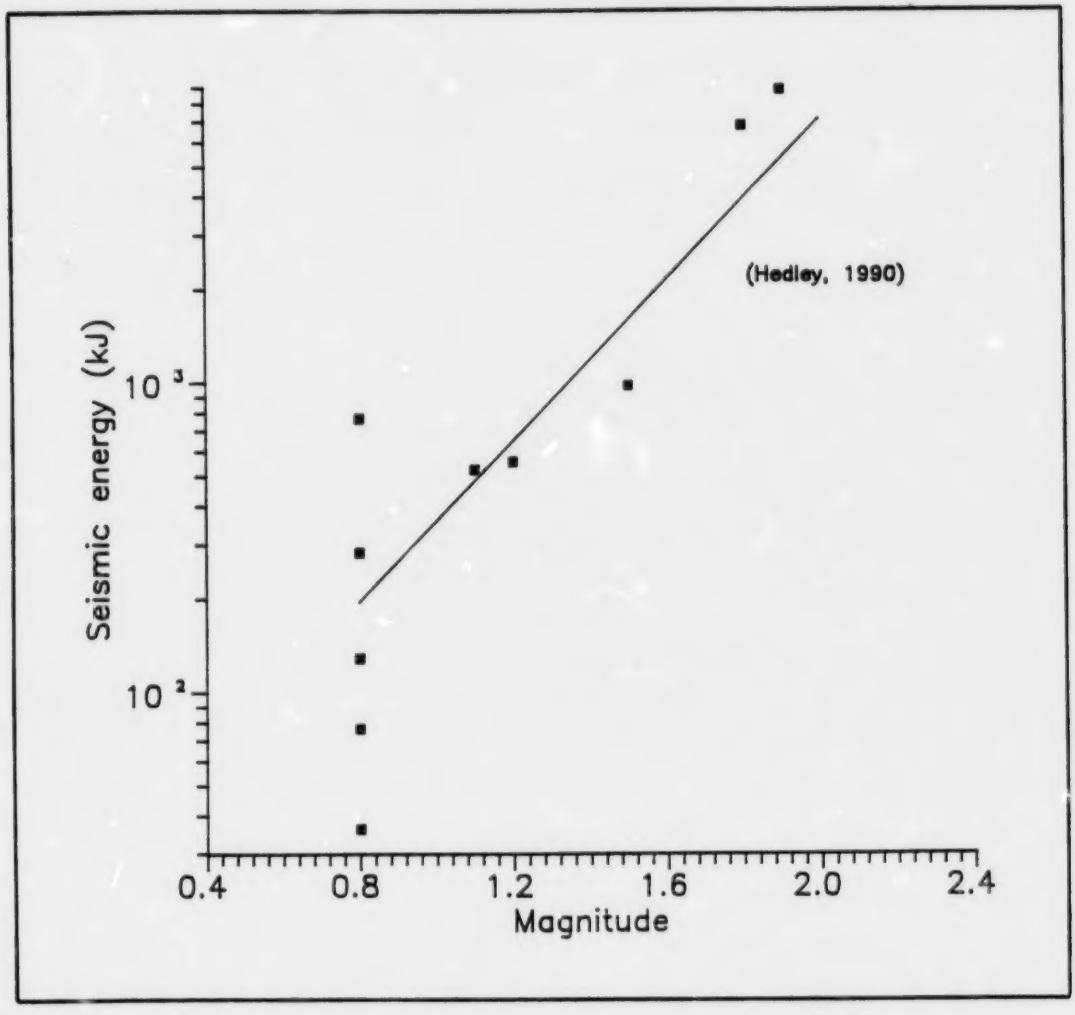

Fig. 8 - Relationship between seismic energy and magnitude.

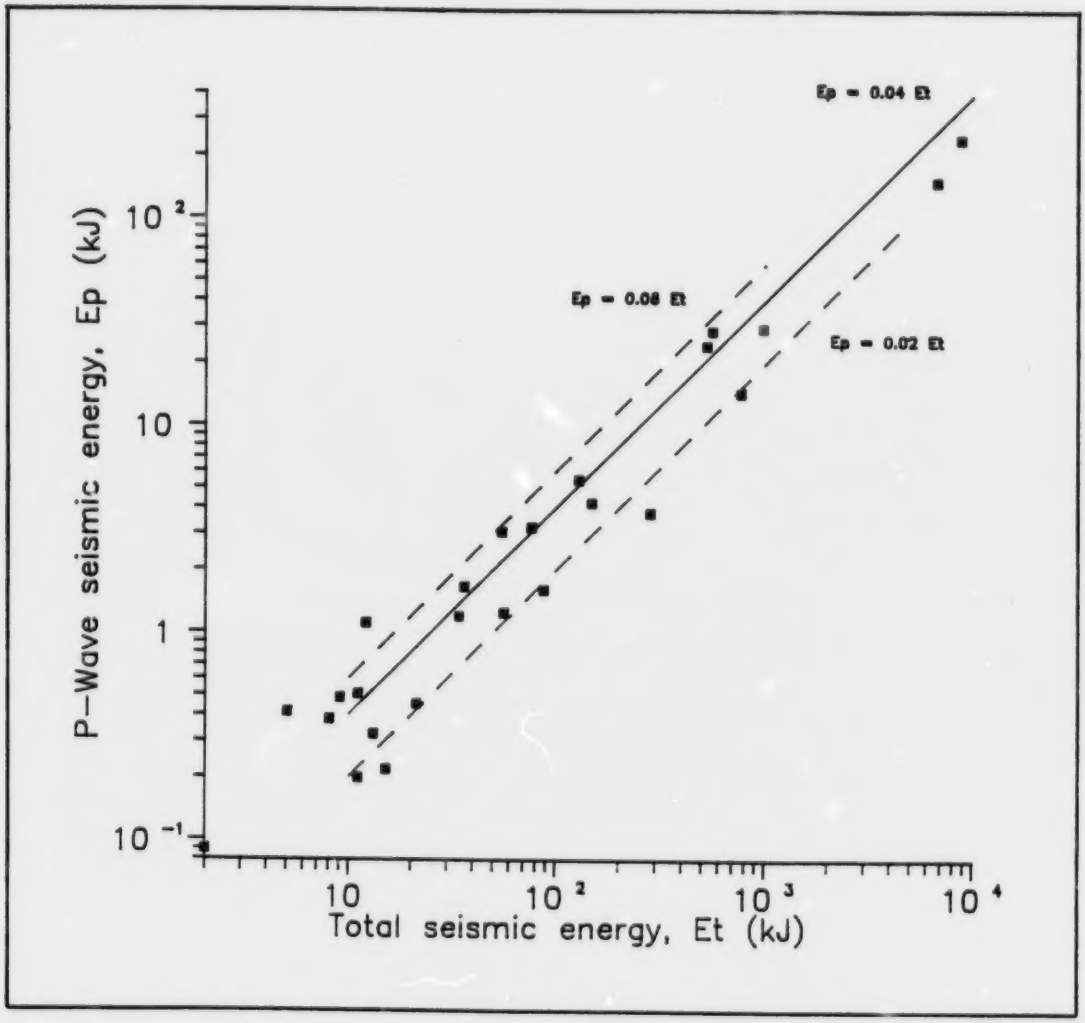

Fig. 9 - Ratio of the seismic energy contained in the P-wave compared to the total seismic energy.

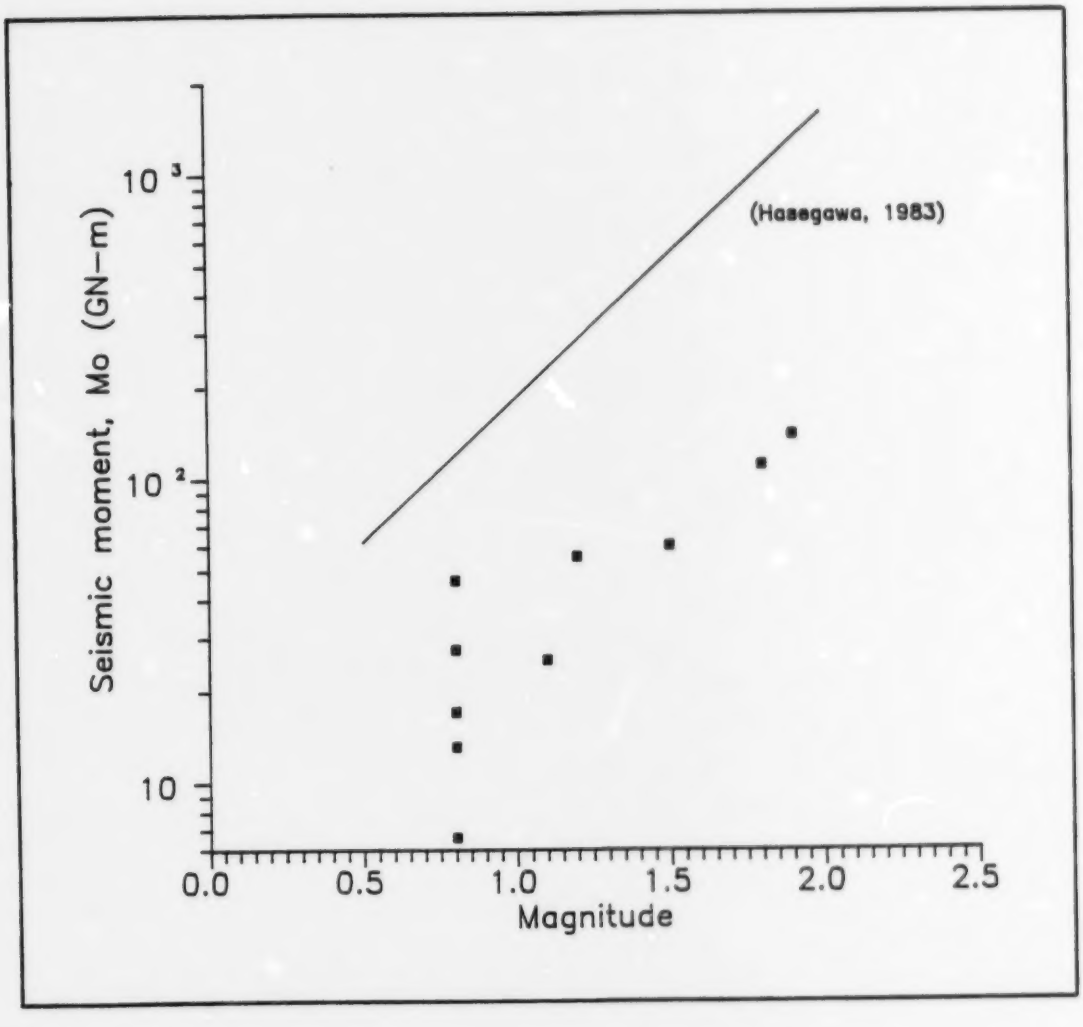

Fig. 10 - Relationship between seismic moment and magnitude.

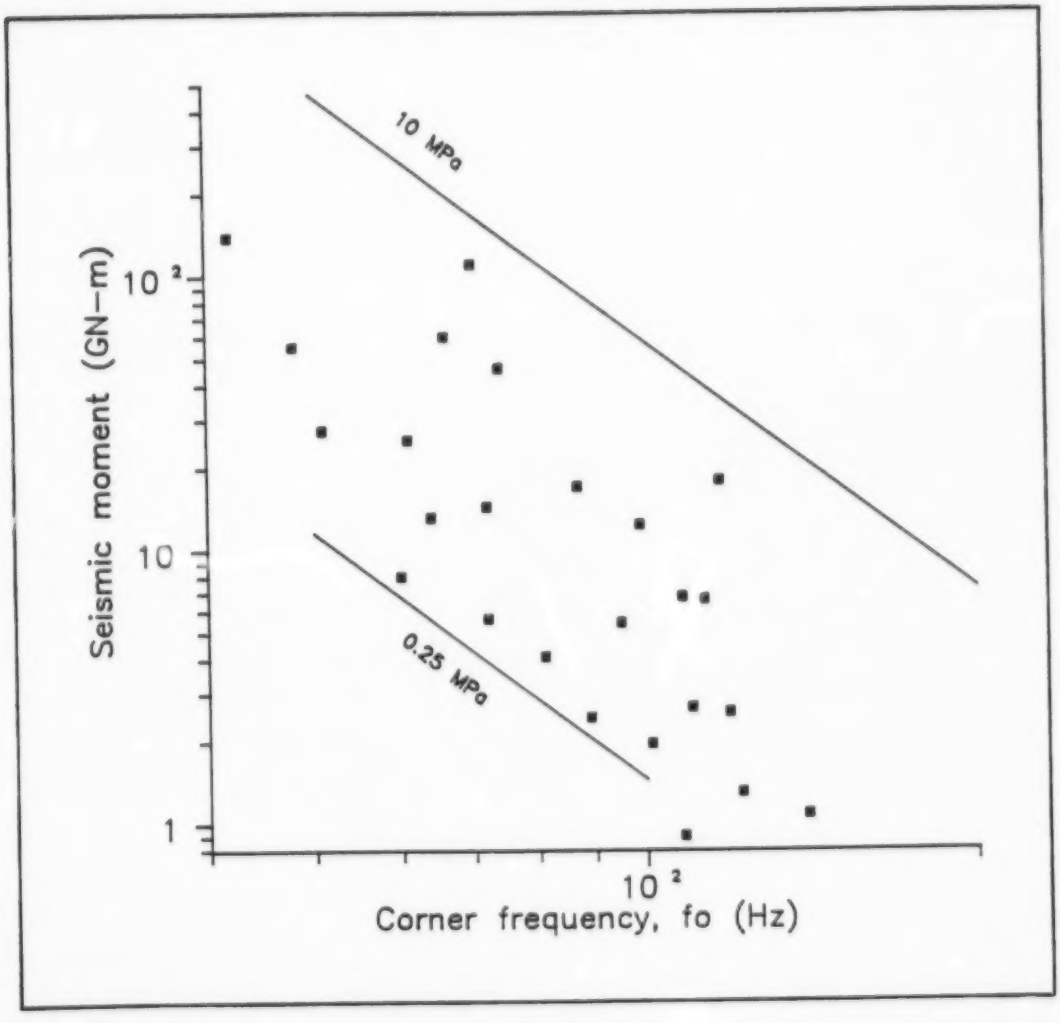

Fig. 11 - Relationship between seismic moment and corner frequency assuming a constant stress drop pattern between 0.25 and 10 MPa.

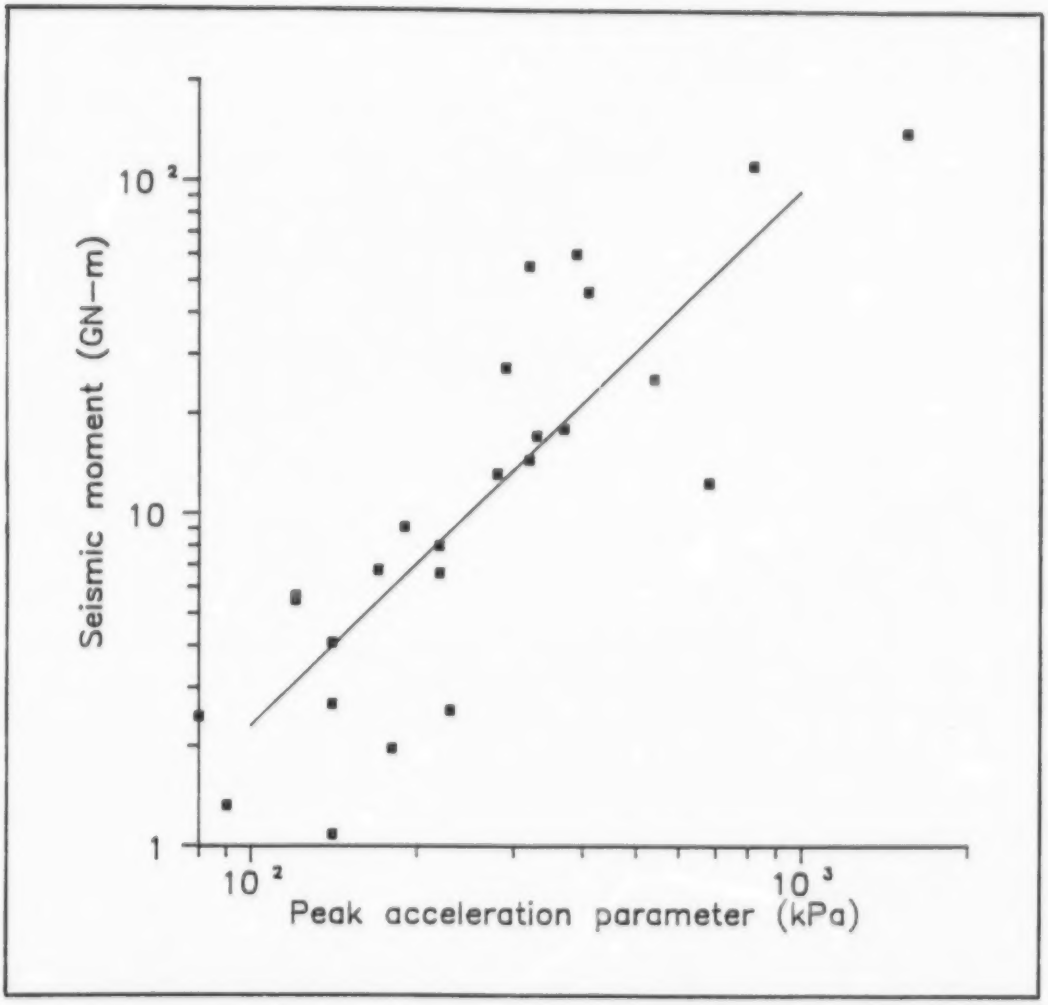

Fig. 12 - Seismic moment as a function of peak acceleration parameter.

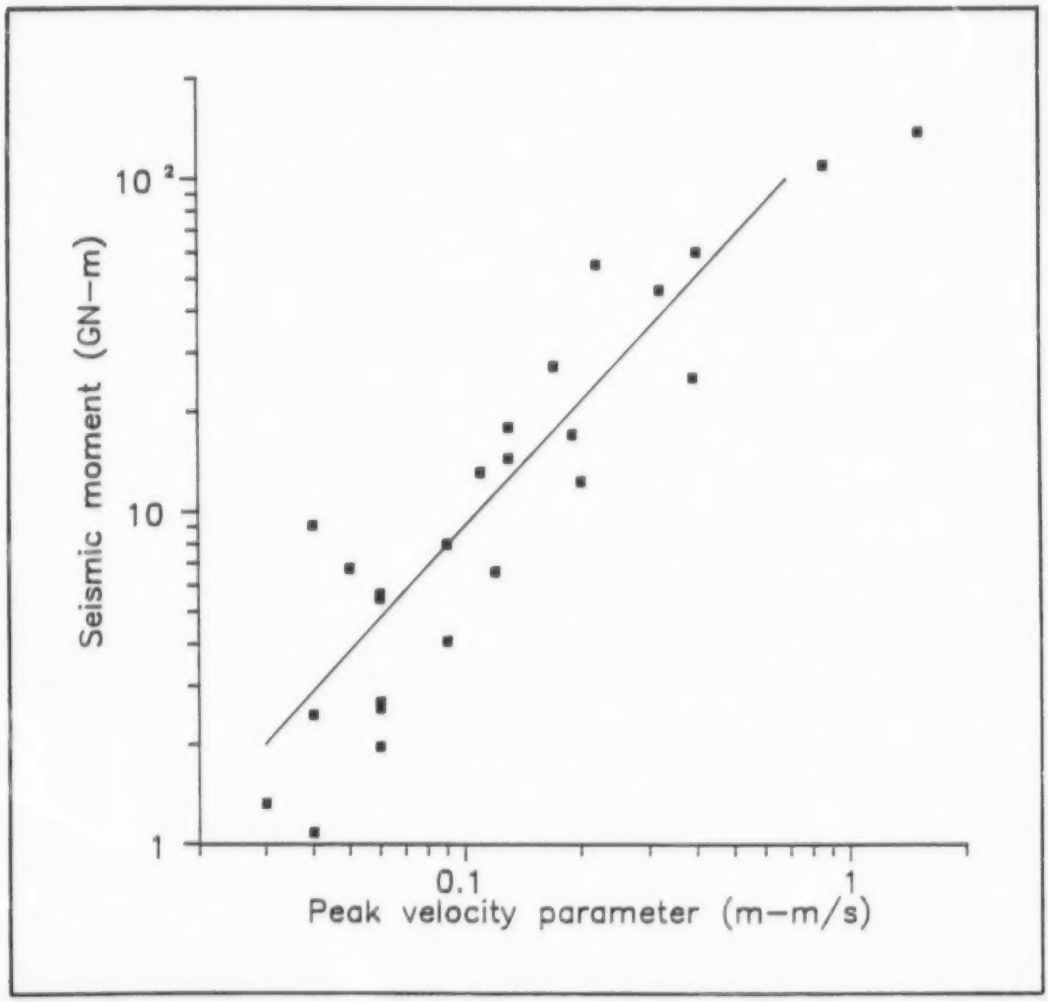

Fig. 13 - Seismic moment as a function of peak velocity parameter.